Sponsored by Gore & Associates

Imaging Considerations for Every Endovascular Aortic Branch Program

With increasing case complexity, proper protocol is crucial.

BY GUSTAVO S. ODERICH, MD, AND GIULIANO SANDRI, MD

Endovascular aneurism repair (EVAR) has been widely accepted as the first treatment option for patients with aortic aneurysms.[1-5] Prospective studies have shown that EVAR reduces mortality and morbidity compared with open surgical repair.[1-3] During the past decade, advancements in endovascular technology have focused on expanding the indications of EVAR to patients with complex aneurysms involving the arch, thoracoabdominal aorta, and iliac bifurcation. Total endovascular repair with branch vessel incorporation has been possible by using fenestrated, branched, and parallel stent grafts. Clinical experience from large tertiary centers has shown that these procedures can be performed with high technical success (> 95%) and with mortality in the range of 1%-5% for pararenal and 4%-10% for thoracoabdominal aortic aneurysms.[6-12] Corresponding with these advancements, there have been significant improvements in imaging capabilities to facilitate pre-procedure planning, device implantation, and immediate assessment of the repair.

Figure 1. Large display monitor with computed tomography angiography fusion using GE® Discovery IGS 740 during deployment of a GORE® EXCLUDER® Thoracoabdominal Branch Endoprosthesis*. The yellow line marks the contour of the aorta and renal-mesenteric arteries, which are also identified by colored rings. Note: the image is digital zoom and not a magnification view.

*Caution: Investigational device. Limited by United States law to investigational use.

SCOPE OF THE PROBLEM

EVAR has been traditionally performed with 2D fluoroscopy using C-arm mobile imaging units. Though procedures can be performed in many patients, significant disadvantages are lower x-ray tube output, potential for x-ray tube overheating, and greater radiation exposure to the patient and personnel. Image quality is also compromised, and in some cases, it may not be adequate. Coupled with the increasing demand for complex endovascular procedures, there is raised awareness about the deleterious effects of radiation exposure. El-Sayed and colleagues reported acute DNA damage to operators and patients during standard and complex EVAR. Although the study did not show direct evidence of stochastic effects (e.g., increased risk of cancer), one can extrapolate that repeated exposure to radiation may result in clinical sequelae.[13]

Radiation exposure can be significantly reduced during EVAR depending on the type of hybrid operating room (OR), imaging equipment, and availability of advanced applications such as computed tomography angiography (CTA) fusion or cone-beam computed tomography (CBCT).[14,15] The dose area product (DAP), measured in $Gy.cm^2$, is the product of absorbed radiation dose, or air kerma (AK), measured in Gy or mGy, by the exposed area. The DAP is directly linked to stochastic effects. Although there is a wide variation in DAP for standard and complex EVAR procedures, newer hybrid ORs have decreased radiation exposure for complex EVAR (Table 1). For example, in some studies with standard EVAR the median DAP was measured as high as 276 $Gy.cm^2$ per case, whereas in others the DAP was as low as 43 $Gy.cm^2$ per case for complex EVAR performed using most advanced imaging units.

HYBRID-ROOM CONCEPT

Hybrid ORs combine optimal imaging with the ideal environment to perform complex open and endovascular operations. These rooms are equipped with modern fixed imaging units that have several advantages such as stronger x-ray tube power (preventing overheating), flat panel detectors (optimizing imaging quality), and

TABLE 1. SELECTED REFERENCES FOR DOSIMETRIC DATA FOLLOWING STANDARD AND COMPLEX EVAR

Author(s)	Year	n	Procedure (subgroup)	Fluoroscopy Time (min)	Median DAP (Gy.cm^2)
Geijier et al[16]	2005	24	EVAR	21.4 (7.4–78.9)*	60.1 (16.6–195)*
Weiss et al[17]	2008	12	EVAR	20.6 (12.6–34.2)†	151.7 (52.1–245.4)†
Weerakkody et al[18]	2008	96	EVAR	21 (16–31)	–
Kalef-Ezra et al[19]	2009	62	EVAR	18 (4.3–75)*	37.4 (9–139)*
Kuhelj et al[20]	2010	172	EVAR	17 (2.9–97.8)*	153 (35–700)*
Jones et al[21]	2010	320	EVAR	29.4 ± 23.3§	46.9 ± 28.4§
Panuccio et al[22]	2011	18	BEVAR (extent II-III)	140.7 ± 64.4§	1,005.7 ± 627.8§
		29	BEVAR (extent IV)	81.9 ± 45.8§	642.5 ± 311.6§
Fossaceca et al[23]	2012	153	EVAR	–	78 (27–370)
Howells et al[24]	2012	630	EVAR	18 (2.4–161)	173 (109–3,343)*
		53	BEVAR/FEVAR	58 (6.7–212)*	320.6 (172.1–2,133.2)
Maurel et al[25]	2012	188	EVAR	9.36 (1.76–67.1)*	30 (4.3–280)*
		54	FEVAR	27.2 (2.1–69.1)*	72.8 (11.0–290.0)*
		20	BEVAR	42.98 (2.38–95.5)*	159.5 (29.8–777.0)*
Peach et al[26]	2012	57	EVAR (non-operator controlled)	20.0 (4.8–49.3)*	69 (19.1–950)*
		65	EVAR (operator-controlled)	16.2 (3.1–51.1)*	49 (12.5–133)*
Walsh et al[27]	2012	111	EVAR	18.5‡	85.8‡
Tacher et al[15]	2013	9	BEVAR/FEVAR (2D)	82 ± 46§	1,188 ± 1,067§
		14	BEVAR/FEVAR (3D)	42 ± 22§	984 ± 581§
		14	BEVAR/FEVAR (fusion)	80 ± 36†	656 ± 457†
Patel et al[28]	2013	26	EVAR	19.5 (14.4–31.5)	97.3 (55.4–167.9)
Blaszak et al[29]	2014	266	EVAR (men)	–	271 (37–1,760)†
		31	EVAR (women)	–	276 (64–625)†
Hertault et al[14]	2014	44	EVAR	10.6 (9.1–14.7)	12.2 (8.7–19.9)
		18	FEVAR	30.7 (20.2–40.5)	43.7 (24.7–57.5)
		20	BEVAR	39.5 (34.8–51.6)	47.4 (37.2–108.2)

Abbreviations: 2D, two-dimensional; 3D, three-dimensional; BEVAR, branched endovascular aortic repair; DAP, dose area product; FEVAR, fenestrated endovascular aortic repair. *Median (range); †Mean (range); ‡Mean; §Mean ± SD. Note: Values are given as mean interquartile range unless otherwise indicated.

customizable protocols to regulate radiation dose levels. Several features such as CTA fusion, CBCT, larger detector panels, digital zoom, and low-dose protocols further reduce the radiation exposure to a patient and an operator.

NOVEL IMAGING APPLICATIONS

CTA Fusion

Fusion imaging using the 3D model is displayed on a large display monitor along with live fluoroscopic imaging (Figure 1). This is used as a 3D "roadmap" to help guide implantation of branched stent grafts by identifying anatomical landmarks without performing repeat 2D angiography (Figure 2). The CTA 3D model and fluoroscopic image are both registered by aligning the two datasets with each other. The 3D model can be obtained from intraoperative, contrast-enhanced CBCT (e.g., CBCT fusion), but this technique has disadvantages since it requires additional radiation exposure, contrast, and is more time consuming. Alternatively, fusion can be created from pre-operative CTA or magnetic resonance angiography (MRA) datasets. CTA fusion has a more efficient workflow and minimizes radiation by avoiding the need to perform CBCT. During the fusion registration workflow, the bone sub-volume from CTA is aligned with two orthogonal fluoroscopic shots using bone landmarks such as the iliac crest and vertebral bodies. Fusion registration workflow can be easily performed by

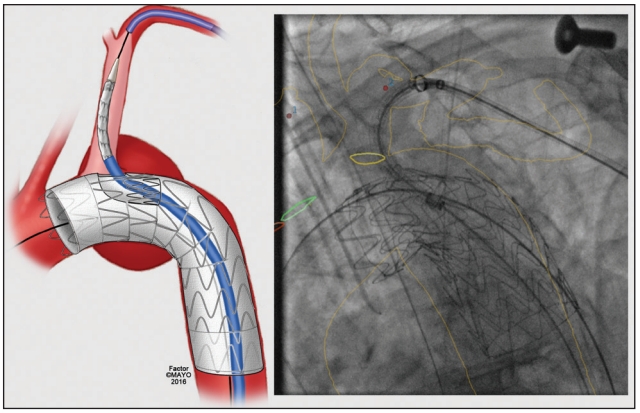

Figure 2. Computed tomography angiography fusion imaging shows vessel outline and origins of the left subclavian (yellow ring) and common carotid arteries (green ring) during deployment of the GORE® TAG® Thoracic Branch Endoprosthesis* to treat distal aortic arch aneurysm. Avoiding repeat angiography markedly reduces contrast use. Used with permission of Mayo Foundation for Medical Education and Research. All rights reserved.

the operator using tableside control and is fast, adding minimal or no radiation exposure.

There is increasing evidence on the benefit of fusion imaging to facilitate standard and complex EVAR.[14,15] Prior reports have shown significant reduction in total dose of contrast media compared with procedures performed with conventional fluoroscopy.[30,31] Hertault et al and Dias et al[14,30] have shown noticeable decline in radiation dose since adoption of CTA fusion.

Cone-Beam Computed Tomography

Complex EVAR has been plagued by high reintervention rates with secondary stent graft-related complications in up to 34% of patients. In some reports, early reinterventions (< 30 days) are required in 10% of patients to treat proximal endoleaks from attachment sites or severe side branch kinks, accounting for nearly half of all reinterventions (Figure 3).[6,9,11,12] The most common problems are endoleaks from sealing zones or compression of side stents. If not recognized, these problems may lead to devastating complications such as stent occlusion or aneurysm rupture.

Traditionally, the immediate assessment of the repair has been done by 2D angiography. However, this may not adequately demonstrate structural problems such as kinks or compression of side branch stents. CBCT with and/or without contrast enhancement using high definition imaging can be obtained through 3D rotation. Multiplanar reconstructions of the CBCT images allow immediate assessment of the repair including location of stent grafts in relation to target vessels, configuration of side branches (Figure 4), patency of iliac limbs, and

*Caution: Investigational device. Limited by United States law to investigational use.

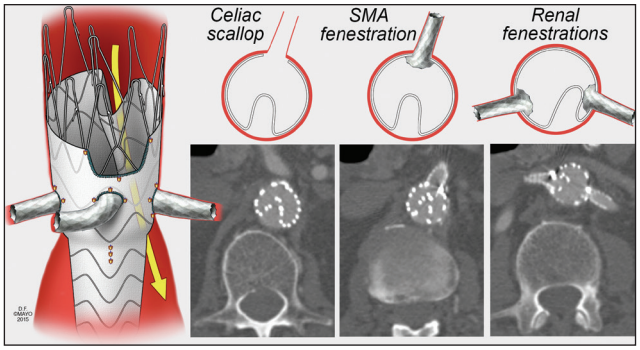

Figure 3. Illustration of a patient who was found to have an in-folded aortic fenestrated stent graft on postoperative computed tomography (CT) angiography. The patient required an early reintervention, which may have been avoided by immediate assessment with cone-beam CT. Used with permission of Mayo Foundation for Medical Education and Research. All rights reserved.

presence of endoleaks. These technical complications can be recognized and immediately revised at the time of the initial procedure (Figures 5 and 6), avoiding potential risk of complications and decreasing the need for secondary reinterventions. Schulz and colleagues recently reported a comparison of contrast-enhanced CBCT (ceCBCT) with digital subtraction angiography (DSA) and post-procedure CTA.[32] In that study, ceCBCT detected more endoleaks (36%) than DSA (16%) and CTA (22%), prompting intraoperative interventions in 7% of patients.

MAYO CLINIC WORKFLOW

All patients undergoing complex EVAR receive preoperative CTA of the chest, abdomen, and pelvis. This is the most important imaging modality to plan EVAR. Its utility relies on the accurate assessment of etiology, extent of disease, involvement of side branches, adequacy

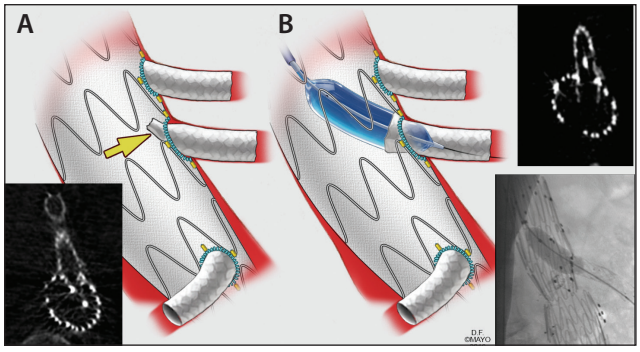

Figure 4. Completion cone-beam CT (CBCT) shows compression of the superior mesenteric artery bridging stent (A, yellow arrow). This was immediately revised by balloon angioplasty (B) with resolution of the compression on repeat CBCT. Used with permission of Mayo Foundation for Medical Education and Research. All rights reserved.

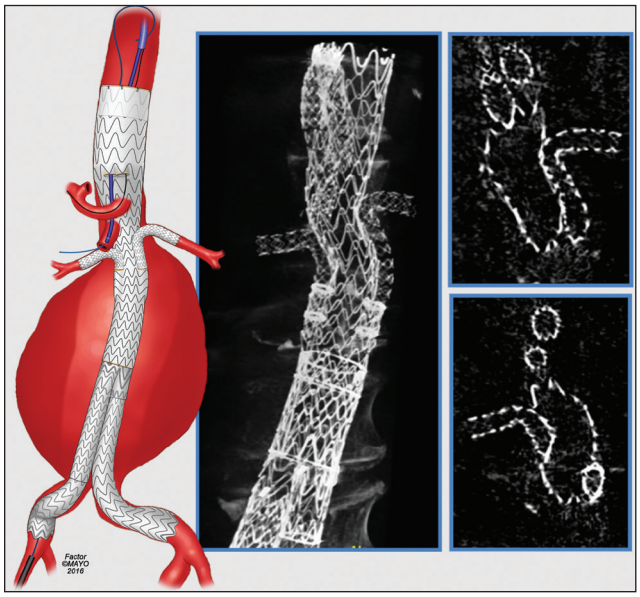

Figure 5. Completion cone-beam CT in a patient treated with a GORE® EXCLUDER® Thoracoabdominal Branch Endoprosthesis stent graft shows stent architecture and absence of kinks within the retrograde renal stents. Used with permission of Mayo Foundation for Medical Education and Research. All rights reserved.

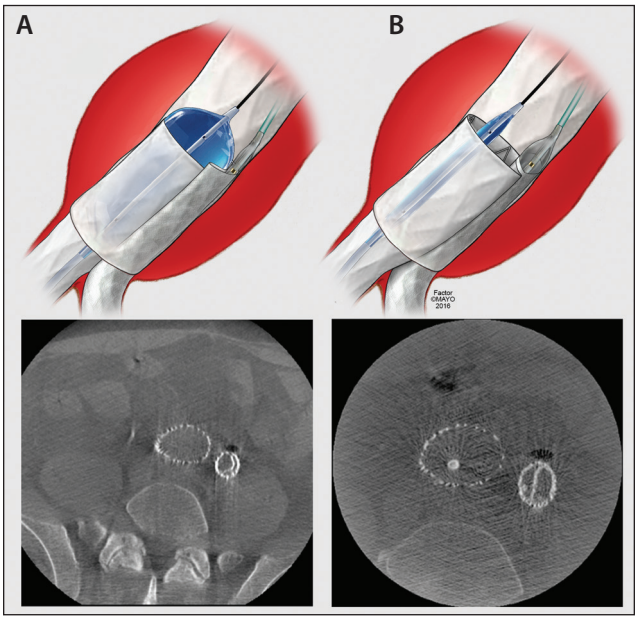

Figure 6. Intraoperative cone-beam CT was used in this patient who was treated with an aortic stent graft and parallel iliac stent grafts. Note compression of the internal iliac bridging stent (A). This was immediately revised by placement of balloon-expandable stents to achieve perfect "D" configuration (B). Used with permission of Mayo Foundation for Medical Education and Research. All rights reserved.

of access vessels, and presence of extravascular diseases that might affect treatment selection and approach. Before the procedure, meticulous planning is reviewed on the GE Advantage Workstation (AW) using the EVAR Assist planning tool. The 3D reconstruction obtained from the preoperative CTA is carefully analyzed for access routes, measurements of lengths, clock positions, and angles of origin for the renal-mesenteric arteries. Colored rings mark the location of each target vessel during preparation of CTA fusion (Figure 1). Ideal angles of parallax view are also stored during the planning phase, allowing the gantry to be positioned at the proper angle during the procedure. Automatic positioning capability contributes to minimizing fluoroscopy time and prevents the need to perform unnecessary DSA runs. Sizing and planning can be done weeks before the procedure and are fully integrated into the imaging unit on the day of the operation.

All complex EVAR cases are currently performed in a dedicated hybrid endovascular room with the latest generation GE® DISCOVERY IGS 740 angiography system. This imaging has a 40 X 40 cm flat panel detector, EVAR Assist software, CTA fusion, and high-definition CBCT. The initial registration process is done using pre-operative CTA, which is fused with two orthogonal views, either anterior-posterior (AP) and lateral or right anterior oblique and left anterior oblique. The CTA bone sub-volume is aligned with the bone landmarks from two fluoroscopic projections. After arterial access is established, the 3D CTA vessel model is realigned by selective catheterization of one of the renal arteries with limited angiography or by DSA using injection of 7 ml of contrast medium at 30 ml/sec. The use of iodinated contrast is minimized throughout the procedure

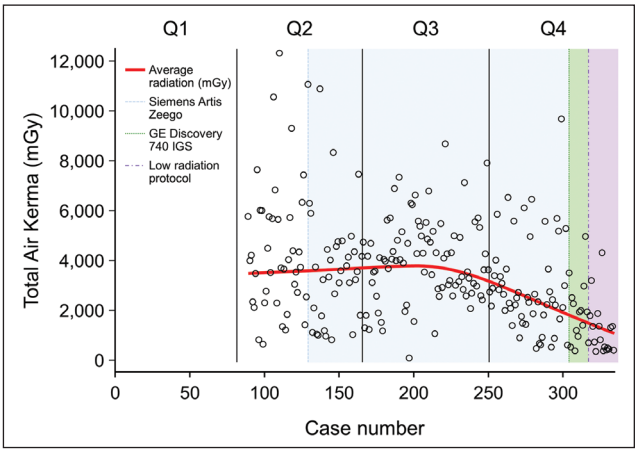

Figure 7. Radiation dose (dots and red line) in 340 consecutive patients treated by fenestrated and branched stent grafts. Radiation dose was recorded after the first quartile of experience (Q1). Note: Marked reduction in radiation exposure after 250 cases. The lowest radiation levels were achieved using the GE® Discovery IGS 740 unit with low-radiation protocol (green and purple panels).

TABLE 2. TECHNICAL TIPS TO MINIMIZE RADIATION DOSE DURING STANDARD AND COMPLEX EVAR

Technical Tip	Comments
Shielding	Lead aprons, thyroid shield, lead goggles, tableside glass shields, and skirts
Tube Position	Avoid lateral and oblique projections
Continuous Monitoring Exposure	Modern fluoroscopy systems display fluoroscopy time, DAP, and cumulative AK; staff exposure should be monitored with active dosimeters that provide direct display of accumulated dose; longitudinal dose analysis should be collected and reviewed on regular basis
Flat Panel Detectors	High level radiographic performance with limited geometric distortion and high uniformity
Pulse Mode	7.5 images per second reduce number of produced images by 90% compared with continuous mode (30 images per second)
Auto Exposing Settings	X-ray exposure is automatically adjusted in real time to deliver constant image quality at lowest dose
Low Dose Setting	Low frame rate and detail settings
Time on Pedal	Pedal control by senior operator with limited time on pedal at all times
Fluoroscopic Mode	Digital subtraction angiography should be avoided and instead high quality fluoroscopic loops should be used to analyze target vessels before and after stenting
Collimation	Reduction of field of view using vertical, horizontal, and iris collimation to focus on the area of interest
Digital Zoom	Digital zoom is applied instead of increased field of view whenever possible
Limit Angulations	Gantry position > 30° oblique or > 15° cranial increases staff exposure to scattered radiation and deteriorate image quality; angled and lateral views should be minimized and used only for short intervals
Imaging Chain Geometry	The detector should be placed as close to the patient as possible
CTA Fusion	Onlay anatomical correlation with 2D fluoroscopy
CBCT	Immediate assessment of technical problems and endoleaks

Abbreviations: 2D, two-dimensional; AK, air kerma; CTA, computed tomography angiography; CBCT, cone-beam computed tomography; DAP, dose area product.

using CTA fusion to identify the target vessels. Once the vessels are located, small hand injections (3 ml of contrast in 7 ml of saline) with fluoro loops are stored for confirmation. We avoid DSA acquisitions to minimize radiation. Once the stent graft has been implanted, CBCT is done with and without contrast-enhancement to assess stent architecture and endoleaks. If there is a significant technical problem, this is immediately revised.

Radiation protection is critical when performing these procedures by following the "as low as reasonably achievable" (ALARA) principle, which aims to use the lowest radiation exposure to complete the procedure. To follow the ALARA principle, several technical tips (Table 2) have been implemented as part of a low dose protocol. The protocol is customized with reduced fluoro frame rate (7.5 fps) with low detail. The fluoroscopic pedal is controlled by the most senior operating surgeon and DSA acquisitions are avoided whenever possible. Increased magnification is avoided by using the digital zoom feature. Gantry angulations are limited to < 30° anterior oblique views and imaging is collimated with digital zooming, instead of magnified views. Proper shielding is used to minimize scattered radiation, including protective garments, eye protection, lead hats, and protective surgical drapes.

CLINICAL RESULTS

Our results have continued to evolve and reflect significant time investment from the physician on planning, performing, and refining the procedure. It is no surprise that for complex EVAR there is a steep learning curve, and increasing clinical experience has been associated with improvements in operative mortality and morbidity. We have recently reviewed our experience with 334 consecutive patients treated by complex EVAR. Operative mortality was 2% for the entire cohort, but declined from 6% in the first quartile to 0% in the last two quartiles of experience. Similarly, we have noted a significant reduction in radiation dose (Figures 7 and 8) since the installation of the latest generation of GE Discovery IGS 740 hybrid endovascular room and adaptation to our low dose protocol. The reduced dose

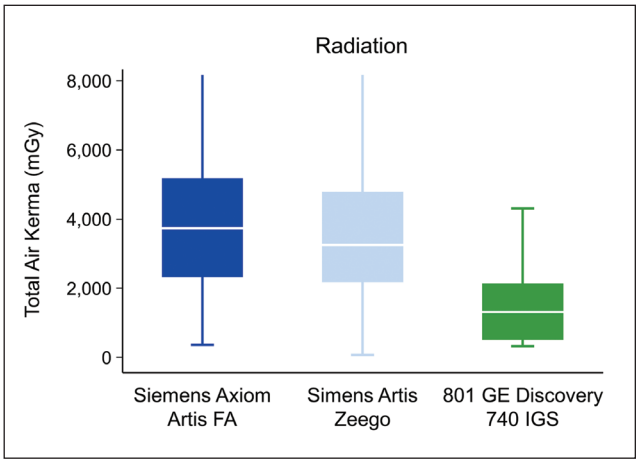

Figure 8. Radiation dose by specific type of imaging unit in patients treated by fenestrated branched stent grafts. The bar marks median and 95% confidence interval, whereas the line marks minimum and maximum value.

in radiation exposure is explained by the use of CTA fusion with fluoroscopic registration (as opposed to initial CBCT) fusion, digital zoom with collimation (as opposed to larger magnification), and fluoro loops (as opposed to DSA acquisitions).

CONCLUSION

Complex EVAR has been increasingly utilized to treat aortic aneurysms involving the aortic arch, thoracoabdominal aorta, and iliac bifurcation. It is important that centers performing these types of procedures are prepared to adapt to the technical demands of newer devices to treat complex anatomy and have advanced imaging tools available. There are several advantages of latest generation hybrid operating rooms, notably the combination of the ideal surgical environment with optimal imaging and advanced applications to minimize radiation exposure, use of contrast media, and need for secondary interventions. ■

1. Lederle FA, Freischlag JA, Kyriakides TC, et al. Long-term comparison of endovascular and open repair of abdominal aortic aneurysm. N Engl J Med. 2012;367:1988-1997.
2. Schermerhorn ML, Buck DB, O'Malley AJ, et al. Long-term outcomes of abdominal aortic aneurysm in the medicare population. N Engl J Med. 2015;373:328-338.
3. Patel R, Sweeting MJ, Powell JT, Greenhalgh RM. Endovascular versus open repair of abdominal aortic aneurysm in 15-years' follow-up of the UK endovascular aneurysm repair trial 1 (EVAR trial 1): a randomised controlled trial. Lancet. 2016;388:2366-2374.
4. Foley PJ, Criado FJ, Farber MA, et al. Results with the Talent thoracic stent graft in the VALOR trial. J Vasc Surg. 2012;56:1214-1221.e1.
5. Matsumura JS, Melissano G, Cambria RP, et al. Five-year results of thoracic endovascular aortic repair with the Zenith TX2. J Vasc Surg. 2014;60:1-10.
6. Mastracci TM, Eagleton MJ, Kuramochi Y, et al. Twelve-year results of fenestrated endografts for juxtarenal and group IV thoracoabdominal aneurysms. J Vasc Surg. 2015;61:355-364.
7. Greenberg R, Eagleton M, Mastracci T. Branched endografts for thoracoabdominal aneurysms. J Thorac Cardiovasc Surg. 2010;140:S171-178.
8. de Souza LR, Oderich GS, Banga PV, et al. Outcomes of total percutaneous endovascular aortic repair for thoracic, fenestrated, and branched endografts. J Vasc Surg. 2015;62:1442-1449.e3.
9. Amiot S, Haulon S, Becquemin JP, et al. Fenestrated endovascular grafting: the French multicentre experience. Eur J Vasc Endovasc Surg. 2010;39:537-544.
10. Oderich G, Ribeiro M, Hofer J, et al. Prospective, nonrandomized study to evaluate endovascular repair of pararenal and thoracoabdominal aortic aneurysms using fenestrated-branched endografts based on supraceliac sealing zones [published online December 13, 2016]. J Vasc Surg.
11. Oderich GS, Ribeiro M, Reis de Souza L, et al. Endovascular repair of thoracoabdominal aortic aneurysms using fenestrated and branched endografts [published online October 22, 2016]. J Thorac Cardiovasc Surg.
12. Eagleton MJ, Follansbee M, Wolski K, et al. Fenestrated and branched endovascular aneurysm repair outcomes for type II and III thoracoabdominal aortic aneurysms. J Vasc Surg. 2016;63:930-942.
13. El-Sayed T, Patel AS, Saha P, et al. Endovascular aortic repair is associated with activation of markers of radiation induced DNA damage in both operators and patients. Eur J Vasc Endovasc Surg. 2016;52:e55.
14. Hertault A, Maurel B, Sobocinski J, et al. Impact of hybrid rooms with image fusion on radiation exposure during endovascular aortic repair. Eur J Vasc Endovasc Surg. 2014;48:382-390.
15. Tacher V, Lin M, Desgranges P, et al. Image guidance for endovascular repair of complex aortic aneurysms: comparison of two-dimensional and three-dimensional angiography and image fusion. J Vasc Interv Radiol. 2013;24:1698-1706.
16. Geijer H, Larzon T, Popek R, Beckman KW. Radiation exposure in stent grafting of abdominal aortic aneurysms. Br J Radiol. 2005;78:906-912.
17. Weiss DJ, Pipinos, II, Longo GM, et al. Direct and indirect measurement of patient radiation exposure during endovascular aortic aneurysm repair. Ann Vasc Surg. 2008;22:723-729.
18. Weerakkody RA, Walsh SR, Cousins C, et al. Radiation exposure during endovascular aneurysm repair. Br J Surg. 2008;95:699-702.
19. Kalef-Ezra JA, Karavasilis S, Ziogas D, et al. Radiation burden of patients undergoing endovascular abdominal aortic aneurysm repair. J Vasc Surg. 2009;49:283-287.
20. Kuhelj D, Zdesar U, Jevtic V, et al. Risk of deterministic effects during endovascular aortic stent graft implantation. Br J Radiol. 2010;83:958-963.
21. Jones C, Badger SA, Boyd CS, Soong CV. The impact of radiation dose exposure during endovascular aneurysm repair on patient safety. J Vasc Surg. 2010;52:298-302.
22. Panuccio G, Greenberg RK, Wunderle K, et al. Comparison of indirect radiation dose estimates with directly measured radiation dose for patients and operators during complex endovascular procedures. J Vasc Surg. 2011;53:885-894.
23. Fossaceca R, Brambilla M, Guzzardi G, et al. The impact of radiological equipment on patient radiation exposure during endovascular aortic aneurysm repair. Eur Radiol. 2012;22:2424-2431.
24. Howells P, Eaton R, Patel AS. Risk of radiation exposure during endovascular aortic repair. Eur J Vasc Endovasc Surg. 2012;43:393-397.
25. Maurel B, Sobocinski J, Perini P, et al. Evaluation of radiation during EVAR performed on a mobile C-arm. Eur J Vasc Endovasc Surg. 2012;43:16-21.
26. Peach G, Sinha S, Black SA, et al. Operator-controlled imaging significantly reduces radiation exposure during EVAR. Eur J Vasc Endovasc Surg. 2012;44:395-398.
27. Walsh C, O'Callaghan A, Moore D, et al. Measurement and optimization of patient radiation doses in endovascular aneurysm repair. Eur J Vasc Endovasc Surg. 2012;43:534-539.
28. Patel AP, Gallacher D, Dourado R, et al. Occupational radiation exposure during endovascular aortic procedures. Eur J Vasc Endovasc Surg. 2013;46:424-430.
29. Blaszak MA, Juszkat R. Monte Carlo simulations for assessment of organ radiation doses and cancer risk in patients undergoing abdominal stent graft implantation. Eur J Vasc Endovasc Surg. 2014;48:23-28.
30. Dias NV, Billberg H, Sonesson B, et al. The effects of combining fusion imaging, low-frequency pulsed fluoroscopy, and low-concentration contrast agent during endovascular aneurysm repair. J Vasc Surg. 2016;63:1147-1155.
31. McNally MM, Scali ST, Feezor RJ, Neal D, Huber TS, Beck AW. Three-dimensional fusion computed tomography decreases radiation exposure, procedure time, and contrast use during fenestrated endovascular aortic repair. J Vasc Surg. 2015;61:309-316.
32. Schulz CJ, Schmitt M, Bockler D, Geisbusch P. Intraoperative contrast-enhanced cone beam computed tomography to assess technical success during endovascular aneurysm repair. J Vasc Surg. 2016;64:577-584.

Gustavo S. Oderich, MD
Professor of Surgery
Director of Endovascular Therapy
Advanced Endovascular Aortic Research Program
Division of Vascular and Endovascular Surgery
Mayo Clinic
Rochester, Minnesota
oderich.gustavo@mayo.edu
Disclosures: Consultant agreements with Gore & Associates, Cook Medical, and Bolton Medical, with all consulting fees paid to Mayo Clinic; research grants received from Cook Medical, Gore & Associates, and GE Healthcare paid to Mayo Clinic.

Giuliano Sandri, MD
Clinical Research Fellow
Advanced Endovascular Aortic Research Program
Division of Vascular and Endovascular Surgery
Mayo Clinic
Rochester, Minnesota
Disclosures: None.